Time-resolved photoelectron imaging of large anionic methanol clusters: $(Methanol)_n^-$ ($n \sim 145-535$)

Aster Kammrath, Graham B. Griffin, Jan R. R. Verlet,[a)]
Ryan M. Young, and Daniel M. Neumark[b)]
Department of Chemistry, University of California, Berkeley, California 94720
and Chemical Sciences Division, Lawrence Berkeley National Laboratory, Berkeley, California 94720

(Received 19 April 2007; accepted 15 May 2007; published online 27 June 2007)

The dynamics of an excess electron in size-selected methanol clusters is studied via pump-probe spectroscopy with resolution of ~120 fs. Following excitation, the excess electron undergoes internal conversion back to the ground state with lifetimes of 260–175 fs in $(CH_3OH)_n^-$ ($n=145-535$) and 280–230 fs in $(CD_3OD)_n^-$($n=210-390$), decreasing with increasing cluster size. The clusters then undergo vibrational relaxation on the ground state on a time scale of 760±250 fs. The excited state lifetimes for $(CH_3OH)_n^-$ clusters extrapolate to a value of 157±25 fs in the limit of infinite cluster size. © *2007 American Institute of Physics*. [DOI: 10.1063/1.2747618]

I. INTRODUCTION

Since its discovery,[1] the hydrated electron has been of fundamental interest in many areas of science spanning chemistry, physics, and biology. As the simplest quantum solute, it is a benchmark system for understanding the physical and chemical bases of solvation. Hydrated electrons play a key role in radiation chemistry and biology:[2] they can be formed in living cells by ionizing radiation and their high reactivity leads to radical formation with significant potential for genetic damage.[3–5] From both perspectives, it is important to have a more complete understanding of the binding motifs and dynamics of the electron solvated in water and other solvents—not only to have a better basis for modeling the behavior of free electrons in cells, but also to gain new and fundamental insights into the nature of the electron-solvent interaction, as expressed in the spectroscopy and dynamics of solvated electrons. Consequently, many studies have been performed on the hydrated electron[6–11] and its cluster counterparts,[12–18] $(water)_n^-$. The solvated electron in liquid methanol has also received considerable experimental[19–22] and theoretical[23–25] attention. However, only very few studies have been made of $(methanol)_n^-$ clusters,[26–28] and here, we present the first studies of time-resolved dynamics in these species.

Experiments on the bulk hydrated electron, based primarily on transient absorption,[29–33] have shown that when the equilibrated solvated electron is photoexcited, relaxation takes place on three time scales: $\tau_1 \sim 30-80$ fs (60–120 fs in D_2O), $\tau_2 \sim 200-300$ fs, and $\tau_3 \sim 1$ ps.[30] These time scales have been variously attributed to localized and extended solvation dynamics on the excited (p) state, internal conversion (IC) to the (s) ground state, and localized and extended solvation on the ground state.[29,30,32] The difficulties attendant to interpreting bulk experiments have inspired attempts to gain further insight through experiments with $(water)_n^-$ clusters using time-resolved photoelectron spectroscopy (TRPES),[34] from which the extraction of excited state lifetimes is more straightforward.

TRPES experiments have shown that for $(water)_n^-$ clusters in the size range $25 \leqslant n \leqslant 100$, initial relaxation proceeds first by IC from the p to s state at ultrafast time scales on the order of 100 fs,[35,36] followed by slower relaxation with two time scales on the ground state.[37] The IC lifetimes depend sensitively on cluster size,[35,36] scaling linearly with $1/n$ and extrapolating to values very close to the fastest time scales observed in the bulk, $\tau_{IC}(\infty)=54\pm30$ fs for $(H_2O)_n^-$ and $\tau_{IC}(\infty)=72\pm22$ fs for $(D_2O)_n^-$. The cluster lifetimes for internal conversion display a distinct isotope effect, while the fastest of the bulk time scales is the only one to do so.[32] The first of the two time scales observed on the cluster ground state (following internal conversion) has been attributed to solvation dynamics within the cluster and takes place with a lifetime on the order of 300 fs,[37] showing little or no dependence on cluster size or isotope, and corresponds well to the second time scale observed for the bulk hydrated electron.

These results strongly support the "nonadiabatic" mechanism for relaxation of the bulk hydrated electron, according to which relaxation proceeds by internal conversion on a time scale of 50 fs, followed by localized, then extended solvation on the ground state.[29,32,38,39] We note that the limited temporal resolution of the cluster studies (~120 fs) does not rule out very fast ($\tau \sim 20$ fs) initial solvation on the excited state.[40] Questions remain, however, as to the validity of drawing conclusions about bulk dynamics from trends observed in medium-sized clusters ($n=25-100$), particularly as it is still uncertain whether the $(water)_n^-$ clusters under consideration bind the excess electron in an internalized state comparable to the bulk motif.[41–46]

In order to gain further insights into the relationship between bulk and cluster dynamics, we have turned to the related system of anionic methanol clusters. The solvation of

[a)]Present address: Department of Chemistry, University of Durham, Durham DH1 3LE, UK.
[b)]Author to whom correspondence should be addressed. Electronic mail: dneumark@berkeley.edu

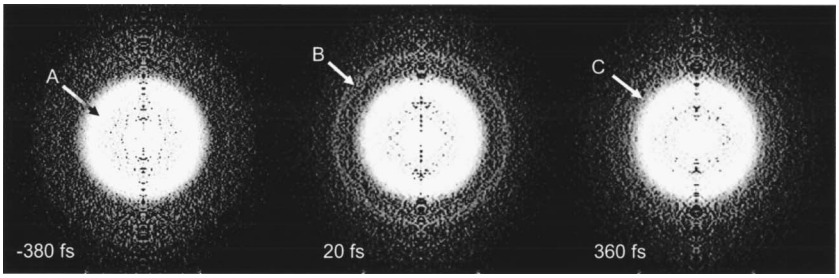

FIG. 1. Transformed images of $(CH_3OD)^-_{265}$ taken with probe-before-pump (−380 fs), during the overlap of the two laser pulses (20 fs), and with probe delayed 360 fs from the pump pulse. Electron kinetic energy increases with the square root of distance from the image center, and different rings correspond to distinct peaks in the photoelectron spectrum.

an electron in bulk methanol is similar to that in water, in that the electron resides in a roughly circular cavity of a few angstroms surrounded by approximately six OH groups,[47] while the ground and first excited states are approximated as an "*s* state" and three "*p* states," respectively, resulting in a single broad, visible absorption feature.[48] The relaxation dynamics of electrons in methanol have been studied theoretically[49] and in time-resolved transient absorption experiments by several groups.[20,22,50–53] The experiments showed substantial variations in the reported time constants, but raised similar issues regarding assignment of the time constants as were found for the hydrated electron. For example, Barbara and co-workers[51,52] found two or three time constants for relaxation, depending on the probe wavelength, with the first time scale observed being the fastest, on the order of 200 fs. They left open the question of whether this first step corresponds to *p*-state solvation or *p*- to *s*-state internal conversion. Thaller *et al.*[53] reported relaxation on three distinct time scales with $\tau_1=105\pm25$ fs, $\tau_2=670\pm100$ fs, and $\tau_3=5.3\pm0.5$ ps, which they assigned to solvent relaxation on the excited *p* state, followed by internal conversion to excited ground state, and finally, solvent relaxation on the ground state, an interpretation in line with the theoretical work by Minary *et al.*[49]

Recent photoelectron (PE) spectroscopy experiments[27] on $(CH_3OH)^-_n$ showed that, just as in $(water)^-_n$, two principal isomers are formed over a wide size range. Methanol II, observed for $n\sim70–460$, exhibits a relatively narrow (~0.25 eV) detachment feature at vertical detachment energies (VDEs) ~0.2–0.5 eV, and is favored at higher backing pressures in the pulsed molecular beam source used to generate the ions. This isomer appears to bind the excess electron in a dipole-bound surface state. Methanol I, favored at lower source pressures, is observed for $n\sim140–460$ with VDEs ~2.0–2.5 eV, displays resonant two-photon detachment at 1.55 eV over the entire size range observed, and has been assigned to an internally solvated electron comparable to the solvated electron in bulk methanol. We have subsequently extended this range well beyond $n=500$ for both isomers, with the same trends continuing at larger cluster sizes. As discussed previously,[27] the assignment of methanol I to internally solvated electrons should be less controversial than in water clusters, because the electron bonding motif proposed for strong surface binding in small water clusters (a unique double-acceptor, double-donor water molecule[54]) is not available for methanol clusters. Furthermore, the methanol clusters are considerably larger than the water clusters hitherto studied. These two considerations imply that dynamical trends in $(methanol)^-_n$ clusters can be more straightforwardly extrapolated to the bulk than those for $(water)^-_n$, thereby providing critical data for comparison.

The current study focuses on dynamics in methanol I clusters. Selected clusters in the size range of $n=145–535$ for $(CH_3OH)^-_n$ [$n=190–390$ for $(CH_3OD)^-_n$ and $n=210–390$ for $(CD_3OD)^-_n$] are studied by time-resolved PE imaging with a temporal resolution of ~120 fs. The excess electron is excited with a pump pulse at 800 nm and detached after a variable delay with a probe pulse at 400 nm. The dynamics following excitation is monitored by tracking changes in the PE spectrum as a function of pump-probe delay.

II. EXPERIMENT

The PE imaging apparatus used in this experiment has been described elsewhere[36,55] and only the details specific to this experiment are given here. Methanol cluster anions are produced by passing argon gas at 5 psi (gauge) through a sample of liquid methanol. The entrained methanol is then expanded through a piezoactuated valve operating at 100 Hz and crossed with an electron beam at ~300 eV. Ions are perpendicularly extracted and mass selected prior to interaction with the laser. The size of the clusters studied ($n=300$ has a mass of ~10 000 amu) is too large for our mass spectrometer to resolve clusters of n and $n\pm1$. All cluster sizes are consequently reported as average values of $n\pm4\%$, with a spread in cluster sizes of $\Delta n\sim2\%$. Experiments were performed on three isotopomers of methanol: CH_3OH, CH_3OD, and CD_3OD.

The fundamental of a chirped-pulse amplified Ti:sapphire system at 800 nm (1.55 eV) with ~80 fs pulse length is used as a pump pulse. Part of the fundamental is split off and doubled (400 nm/3.10 eV) to be used as the probe pulse. Pump-probe delays are set by aligning the pump pulse onto a computer-controlled translation stage. Data are collected over 50 000–80 000 laser shots, with one to six photoelectrons obtained per laser shot, depending on cluster size. Photodetached electrons are collected by velocity map imaging[56] and the photoelectron kinetic energy distribution is reconstructed using the basis set expansion (BASEX) method.[57]

III. RESULTS

Figure 1 shows transformed images taken from $(CH_3OD)^-_{265}$, where electron kinetic energy (eKE) increases with the square root of radius from the image center. At delays where the probe precedes the pump (−380 fs), a single, strong detachment feature A is observed. When the

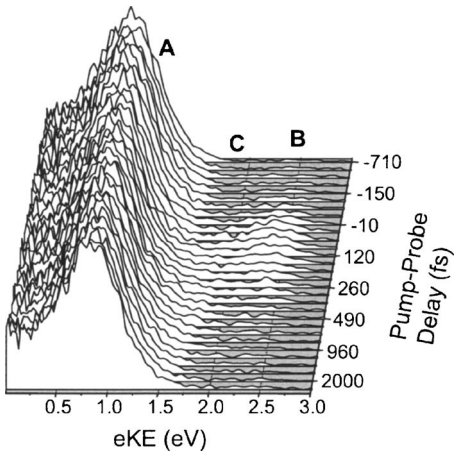

FIG. 2. Time resolved photoelectron spectrum of $(CH_3OD)^-_{265}$ with electron kinetic energy on the horizontal axis and pump-probe delay increasing from back to front.

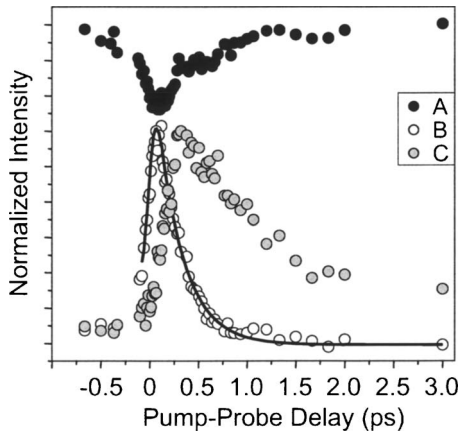

FIG. 3. Normalized intensity of signal integrated over feature A (black circles), through the center of feature B (open circles), and through feature C (shaded circles) shown for $(CD_3OD)^-_{265}$. The solid line through the data from feature B is an analytical fit.

pump overlaps with the probe, a second, much weaker feature B appears. As the delay between pump and probe becomes increasingly positive, the ring corresponding to feature B fades, and the edge of the ring corresponding to feature A becomes less distinct, indicating a shoulder (feature C). Similar dynamics are observed for all clusters sizes of each isotopomer studied.

The evolution of these three features can be clearly distinguished and quantified in the corresponding time-resolved PE spectrum, shown in Fig. 2, with eKE on the horizontal axis and increasing pump-probe delay from back to front. We attribute the intensity at low eKE (<200 meV) to direct detachment by the pump pulse at 1.55 eV, while feature A is assigned to direct detachment by the probe pulse at 3.1 eV, with some contribution from resonant two-photon detachment by the pump pulse. As the pump pulse is delayed to overlap with the probe pulse, feature B appears at about 2.4 eV. At pump-probe delays slightly longer than the start of feature B, feature C becomes apparent as a high-energy shoulder to feature A. Feature B decays quickly without shifting in energy. Feature C decays more slowly than B, during which time its high-eKE edge recedes to lower eKE, until by ~2 ps it is no longer distinguishable from feature A.

The relative integrated intensities of these features as a function of pump-probe delay are shown in Fig. 3 for $(CD_3OD)^-_{265}$. The open circles correspond to feature B (2.1–2.8 eV), while the solid line is an analytical fit (Sec. IV). Shaded and black circles correspond to feature C (1.5–2.0 eV) and a slice through the center of feature A (0.5–1.2 eV), respectively. Feature B reaches a maximum intensity within the cross correlation of the laser pulses and decays virtually to zero by 500 fs. The intensity of feature C reaches a maximum about midway through the decay of feature B, growing at a rate similar to the decay in feature B, after which it decays on a time scale of ~1 ps. At short times, feature A drops in intensity as feature B rises, and recovers partially as feature B decays. It then mostly levels off for several hundred femtoseconds, after which it resumes recovery on a time scale similar to the decay of feature C.

IV. ANALYSIS AND DISCUSSION

A. Assignment of features in $(MeOH)^-_n$ clusters

Feature B is fitted by the convolution of a Gaussian (representing the cross correlation of the laser pump and probe pulses) with a simple exponential decay function of the form

$$I_B(t) = A_0, \quad t < 0,$$
$$I_B(t) = A_1 + A_2 \exp(-t/\tau_B), \quad t \geq 0, \tag{1}$$

where $I_B(t)$ is the integrated intensity over feature B at pump-probe delay time t, $A_{0,1}$ are constants accounting for any offset due to noise, A_2 is the amplitude of the feature, and τ_B is its lifetime.

The lifetimes τ_B obtained are shown in Fig. 4 as a function of cluster size with $(CH_3OH)^-_n$ as black diamonds, $(CH_3OD)^-_n$ as open diamonds, and $(CD_3OD)^-_n$ as gray diamonds, with uncertainties as noted in the caption. Lifetimes are observed to decrease with increasing cluster size for all three isotopomers. No significant isotope effect is observed in τ_B between $(CH_3OH)^-_n$ and $(CH_3OD)^-_n$. The lifetimes for the fully deuterated clusters are consistently longer by an average of 25%. Although the lifetimes for $(CH_3OH)^-_n$ and

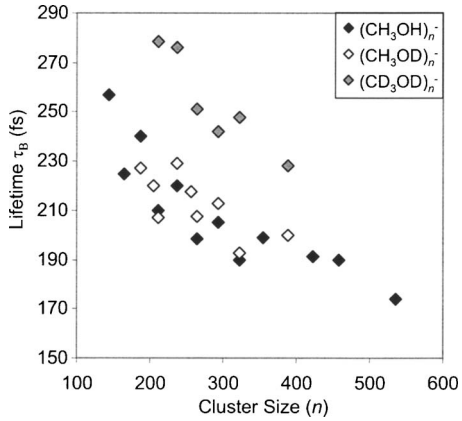

FIG. 4. Lifetimes of feature B as a function of cluster size for $(methanol)^-_n$ with isotopomers as indicated in the legend. Errors are estimated as 15% for $(CH_3OH)^-_n$ and $(CH_3OD)^-_n$ and at 10% for $(CD_3OD)^-_n$.

$(CD_3OD)_n^-$ are mostly within the combined error of each other, the systematically longer lifetimes for $(CD_3OD)_n^-$ suggest a non-negligible isotope effect, as discussed further below.

The decay of feature C is fitted to a simple exponential decay beginning at delays corresponding roughly to the disappearance of feature B according to

$$I_C(t) = A_4 + A_5 \exp(-(t-t_1)/\tau_C), \quad t \geq t_1, \tag{2}$$

where $I_C(t)$ is the integrated intensity over feature C at pump-probe delay time t, t_1 is the delay at which fitting begins, A_4 is a constant accounting for any offset, A_5 is the amplitude of the feature, and τ_C is its lifetime. Lifetimes of $\tau_C = 760 \pm 250$ fs are obtained, showing no consistent or significant change with cluster size or isotope substitution.

The decay of feature B is most logically attributed to the lifetime of the excited p state. Decay may occur via IC to the s state or by excited state autodetachment (ESAD), both of which were observed for $(water)_n^-$ clusters.[36] The experimental signatures used to distinguish the two processes have been outlined in detail previously.[36,58] Briefly, ESAD is manifested as signal from the pump pulse at low eKE, rising with the same time constant as the decay of the excited state feature. In the case of $(methanol)_n^-$ clusters, this signal would be at eKE $<$ 200 meV. We observed a slight increase in the photoelectron intensity in this region during the cross correlation of the laser pulses, after which it levels off, showing no further increase with the decay of feature B. This initial increase is associated with the pump-probe delay becoming positive, at which point the ground state is no longer depleted by the probe pulse before the pump pulse arrives, and does not indicate autodetachment. On the other hand, the recovery of intensity in feature A with the decay of feature B also argues for return of population to the ground electronic state rather than ESAD.

Hence, decay of feature B is assigned to internal conversion from the p state to the s state, and feature C is attributed to vibrationally excited s-state population. We henceforth set $\tau_B = \tau_{IC}$ and assign the decay of feature C to vibrational relaxation on the ground state. The residual intensity left in feature C after ~3 ps is reproducible and indicates that another mechanism (such as more extended vibrational relaxation or evaporation) must become active for the cluster to fully relax. However, we have been unable to directly observe this third step in the relaxation process.

We have considered an alternative interpretation, namely, that feature B represents vibrationally excited p-state population and feature C decays by internal conversion to the s state, but find it inconsistent with our results. First, if feature C is due to detachment of relaxed p-state population, it is difficult to account for its smooth shift to lower eKE—usually indicative of (adiabatic) vibrational relaxation rather than an (nonadiabatic) internal conversion to a lower electronic state. Similarly, if feature B were due to excited p-state population vibrationally relaxing to give feature C, then it is expected to shift in eKE over time, which it does not. The time evolution of both features, therefore, supports their assignment to population decay and ground state vibrational relaxation, respectively.

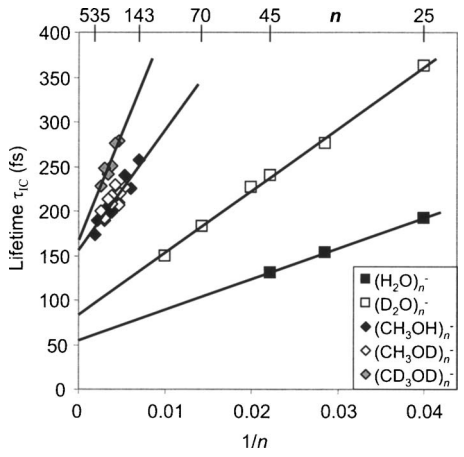

FIG. 5. Internal conversion lifetimes for $(methanol)_n^-$ compared to $(water)_n^-$ as indicated in the legend, plotted as a function of inverse cluster size, $1/n$. Errors are estimated at 10% for both water isotopomers and $(CD_3OD)_n^-$ and at 15% for the other two methanol isotopomers.

B. Comparison with $(water)_n^-$ and bulk solvents

In Fig. 5, the IC time constants τ_{ICM} for $(methanol)_n^-$ are plotted versus $1/n$ for comparison with τ_{IC} of $(water)_n^-$ (τ_{ICW}) previously reported.[36] In Fig. 5 and throughout the rest of this discussion, we refer exclusively to the more tightly bound of the two principal water cluster isomers (water I).[41] The linear correlation between τ_{ICM} and $1/n$ is not as perfect as that of τ_{ICW} to $1/n$, and data are available for only a relatively narrow range on the abscissa (less than a third of the length covered by the water data), making the slope of any linear fit highly uncertain. However, it appears that a correlation does exist between τ_{ICM} and $1/n$, and since the methanol data extend nearly to zero ($n=535$ gives $1/n \sim 0.002$), the intercept is determined with precision comparable to that for the water data despite the larger uncertainty in the slopes. We note that Fischer and Dietz[59] has recently proposed a model based on long range, dipolar coupling between the $p \rightarrow s$ electronic transition and IR active vibrational modes that yields a $1/n$ dependence for the size-dependent lifetimes in $(H_2O)_n^-$ clusters.

Several interesting observations may be drawn from Fig. 5. First, IC lifetimes in methanol are much longer than in water and depend much more steeply on cluster size than in water. Fitting yields a slope of $(13 \pm 6$ ps$)n$ for $(CH_3OH)_n^-$ with an intercept of 157 ± 25 fs compared to a slope of $(3.5 \pm 1.7$ ps$)n$ and an intercept of 54 ± 30 fs for $(H_2O)_n^-$ [$(7.8 \pm 1.1$ ps$)n$ and 72 ± 22 fs for $(D_2O)_n^-$]. For $(CD_3OD)_n^-$, we obtain a slope of $(24 \pm 18$ ps$)n$, with an intercept of 167 ± 66 fs.

The intercepts obtained above correspond to the excited state lifetime in an infinitely sized cluster, $\tau_{IC}(\infty)$, and should thus be compared to results for electrons in bulk methanol. Our value of 157 fs is in striking agreement with the theoretical value of about 150 fs obtained by Zharikov and Fischer[39] for electrons in methanol using a continuum solvated electron model, which also recovers the 50 fs lifetime for the p state observed in the bulk for water.[29] Our extrapolations for methanol and water are also in qualitative agreement with calculations of Borgis *et al.*[60] which predict that

the nonadiabatic transition from the *p* state of the *s* state is 2.7–4.3 times slower in methanol than in water, depending on the method used for the calculation. However, these calculated transition times are for the *equilibrated p*-state electron, and thus apply, in principle, only after excited state solvation has occurred. Since we do not observe *p*-state vibrational relaxation in this experiment (possibly due to insufficient temporal resolution, as mentioned in the Introduction), it is not clear how directly these calculations may be compared to the present results.

Our time constants $\tau_{IC}(\infty)$ of 157 ± 25 fs for the excited state and $\tau_C=760\pm250$ fs, attributed to ground state vibrational relaxation, are also in good agreement with the first two time scales reported by Thaller *et al.*,[53] $\tau_1=105\pm25$ fs and $\tau_2=670\pm100$ fs. The fastest lifetime obtained by the extrapolation of data in this study is slightly longer than expected, if the cluster dynamics mirror those in the bulk. However, the correspondence is close enough to suggest that the fastest time constant reported for the electrons in liquid methanol is, in fact, from internal conversion, just as for water, and does not correspond to relaxation on the excited state.

That $(CH_3OH)_n^-$ and $(CH_3OD)_n^-$ should undergo internal conversion at the same rate is puzzling when one considers that extrapolation of the data for $(D_2O)_n^-$ yields bulk internal lifetimes ~1.4 times as long as for $(H_2O)_n^-$. However, it is consistent with the study by Silva *et al.*[52] of the solvated electron in bulk CH_3OH and CH_3OD, which displays no significant isotope effect in the fastest time scale observed. The two experiments suggest that in methanol, the OH vibrational modes do not dominate in determining internal conversion rates—an interpretation consistent with a theoretical study by Borgis *et al.*,[60] in which they observed that all vibrational modes "contribute almost equally to the overall rate." For water, the OH stretching modes naturally dominate. For methanol, however, a majority of the vibrational modes involve the methyl group. Specifically, Borgis *et al.*[60] note a very strong contribution to the nonadiabatic coupling in a spectral region ($1100-1500\ cm^{-1}$) that includes both the CH_3 deformation and C–O stretch as well as the OH bend.[21] This may be the basis of why $(CD_3OD)_n^-$ should undergo internal conversion more slowly than $(CH_3OH)_n^-$ or $(CH_3OD)_n^-$ and why the overall isotope effect should be less pronounced than in water.

Another notable aspect of the isotope effect in both systems is that it tends to decrease with increasing cluster size over the range of cluster sizes where data are available for both isotopes. For $(water)_n^-$ with $n=25-45$, lifetimes in D_2O are ~1.8–2.0 times as long as in H_2O, while in the bulk, the difference is only about 1.4 times.[29] Similarly for methanol, internal conversion in $(CD_3OD)_n^-$ ($n=210-390$) takes ~1.12–1.35 times as long as in the corresponding $(CH_3OH)_n^-$ clusters, but extrapolation to the bulk gives a smaller ratio of ~1.05 times as long [though the large uncertainty in the slope and intercept for $(CD_3OD)_n^-$ makes these ratios less certain than those observed for water]. It remains to be seen whether this overall effect can be reproduced by the models being developed to explain the excited state lifetimes in clusters.[59]

V. CONCLUSION

Clusters of $(methanol)_n^-$ ($n=145-535$) have been observed to undergo relaxation following excitation of the excess electron on two time scales. The first is assigned to internal conversion from the excited *p* state to the ground *s* state with lifetimes, τ_{IC}, on the order of 170–270 fs, decreasing with cluster size and showing a slight isotope effect for CD_3OD compared to the singly deuterated and fully protonated isotopomers. The second is assigned to solvent relaxation on the ground state with lifetime, $\tau_C\sim760$ fs, showing no significant dependence on isotope substitution or cluster size. These results support assignment of the fastest reported time constants for solvated electrons in bulk methanol to the excited state lifetime rather than relaxation dynamics on the excited state.

The dynamics observed in the present study of $(methanol)_n^-$ for $n=145-535$ shows striking similarity to the dynamics observed in $(water)_n^-$ clusters in the smaller size range of $n=25-100$. Moreover, in both cases, a linear correlation is observed between τ_{IC} and $1/n$, and extrapolation to the bulk limit yields ultrafast lifetimes for the excited *p* state of the excess electron, with values of 157 and 50 fs for methanol and water, respectively, in reasonable agreement with both theoretical predictions and experimental work done on the corresponding bulk systems. Taken together, these results support the perspective that trends observed in the study of size-selected clusters may be used to gain new insights into the complex dynamics of bulk systems.

It will be of interest to determine if the pattern of dynamics and the dependence of internal conversion rates on inverse cluster size are a property of polar solvents in general, or if they depend crucially on the presence of the hydroxyl group present in both water and methanol. To this end, time-resolved studies on $(CH_3CN)_n^-$ clusters are currently underway in our laboratory.

ACKNOWLEDGMENT

This research was funded by the National Science Foundation under Grant No. CHE-0350585.

[1] E. J. Hart and J. W. Boag, J. Am. Chem. Soc. **84**, 4090 (1962).
[2] C. von Sonntag, *The Chemical Basis of Radiation Biology* (Taylor & Francis, London, 1987).
[3] H. Schussler, S. Navaratnam, and L. Distel, Radiat. Phys. Chem. **73**, 163 (2005).
[4] Y. Zheng, P. Cloutier, D. J. Hunting, L. Sanche, and J. R. Wagner, J. Am. Chem. Soc. **127**, 16592 (2005).
[5] J. Simons, Acc. Chem. Res. **39**, 772 (2006).
[6] E. J. Hart and M. Anbar, *The Hydrated Electron* (Wiley-Interscience, New York, 1970).
[7] L. Kevan, Acc. Chem. Res. **14**, 138 (1981).
[8] J. Schnitker, K. Motakabbir, P. J. Rossky, and R. Friesner, Phys. Rev. Lett. **60**, 456 (1988).
[9] B. J. Schwartz and P. J. Rossky, J. Chem. Phys. **101**, 6917 (1994).
[10] A. Migus, Y. Gaudeul, J. L. Martin, and A. Antonetti, Phys. Rev. Lett. **58**, 1559 (1987).
[11] M. Assel, R. Laenen, and A. Laubereau, J. Chem. Phys. **111**, 6869 (1999).
[12] J. V. Coe, G. H. Lee, J. G. Eaton, S. T. Arnold, H. W. Sarkas, K. H. Bowen, C. Ludewigt, H. Haberland, and D. R. Worsnop, J. Chem. Phys. **92**, 3980 (1990).
[13] J. M. Weber, J. Kim, E. A. Woronowicz, G. H. Weddle, I. Becker, O. Cheshnovsky, and M. A. Johnson, Chem. Phys. Lett. **339**, 337 (2001).

[14] J. R. Roscioli, N. I. Hammer, and M. A. Johnson, J. Phys. Chem. A **110**, 7517 (2006).
[15] P. Ayotte and M. A. Johnson, J. Chem. Phys. **106**, 811 (1997).
[16] J. V. Coe, Int. Rev. Phys. Chem. **20**, 33 (2001).
[17] H. M. Lee, S. Lee, and K. S. Kim, J. Chem. Phys. **119**, 187 (2003).
[18] R. N. Barnett, U. Landmann, C. L. Cleveland, and J. Jortner, J. Chem. Phys. **88**, 4429 (1988).
[19] M. C. J. Sauer, S. Arai, and L. M. Dorfman, J. Chem. Phys. **42**, 708 (1965).
[20] C. Pepin, T. Goulet, D. Houde, and J.-P. Jay-Gerin, J. Phys. Chem. **98**, 7009 (1994).
[21] M. J. Tauber, C. M. Stuart, and R. A. Mathies, J. Am. Chem. Soc. **126**, 3414 (2004).
[22] T. Scheidt and R. Laenen, Chem. Phys. Lett. **371**, 445 (2003).
[23] J. Zhu and R. I. Cukier, J. Chem. Phys. **98**, 5679 (1993).
[24] K. Fueki, D.-F. Feng, and L. Kevan, Chem. Phys. Lett. **10**, 504 (1971).
[25] A. A. Mosyak, P. J. Rossky, and L. Turi, Chem. Phys. Lett. **282**, 239 (1998).
[26] L. Turi, J. Chem. Phys. **110**, 10364 (1999).
[27] A. Kammrath, J. R. R. Verlet, G. B. Griffin, and D. M. Neumark, J. Chem. Phys. **125**, 171102 (2006).
[28] C. Desfrancois, H. Abdoul-Carime, N. Khefila, J. P. Schermann, V. Brenner, and P. Millie, J. Chem. Phys. **102**, 4952 (1995).
[29] M. S. Psenichnikov, A. Baltuska, and D. A. Wiersma, Chem. Phys. Lett. **389**, 171 (2004).
[30] A. Thaller, R. Laenen, and A. Laubereau, Chem. Phys. Lett. **398**, 459 (2004).
[31] M. Assel, R. Laenen, and A. Laubereau, Chem. Phys. Lett. **317**, 13 (2000).
[32] K. Yokoyama, C. Silva, D. H. Son, P. K. Walhout, and P. F. Barbara, J. Phys. Chem. A **102**, 6957 (1998).
[33] Y. Kimura, J. C. Alfano, P. K. Walhout, and P. F. Barbara, J. Phys. Chem. **98**, 3450 (1994).
[34] A. Stolow, A. E. Bragg, and D. M. Neumark, Chem. Rev. (Washington, D.C.) **104**, 1719 (2004).
[35] A. E. Bragg, J. R. R. Verlet, A. Kammrath, O. Cheshnovsky, and D. M. Neumark, Science **306**, 669 (2004).
[36] A. E. Bragg, J. R. R. Verlet, A. Kammrath, O. Cheshnovsky, and D. M. Neumark, J. Am. Chem. Soc. **127**, 15283 (2005).
[37] D. H. Paik, I.-R. Lee, D.-S. Yang, J. S. Baskin, and A. H. Zewail, Science **306**, 672 (2004).
[38] A. Hertwig, H. Hippler, A. N. Unterreiner, and P. Vohringer, Ber. Bunsenges. Phys. Chem. **102**, 805 (1998).
[39] A. A. Zharikov and S. F. Fischer, J. Chem. Phys. **124**, 054506 (2006).
[40] P. O. J. Scherer and S. F. Fischer, Chem. Phys. Lett. **421**, 427 (2006).
[41] J. R. R. Verlet, A. E. Bragg, A. Kammrath, O. Cheshnovsky, and D. M. Neumark, Science **307**, 93 (2005).
[42] J. R. R. Verlet, A. E. Bragg, A. Kammrath, O. Cheshnovsky, and D. M. Neumark, Science **310**, 1769b (2005).
[43] L. Turi, W.-S. Sheu, and P. J. Rossky, Science **309**, 914 (2005).
[44] L. Turi, W.-S. Sheu, and P. J. Rossky, Science **310**, 1769c (2005).
[45] A. Kammrath, J. R. R. Verlet, G. B. Griffin, and D. M. Neumark, J. Chem. Phys. **125**, 076101 (2006).
[46] J. R. R. Verlet, A. Kammrath, G. B. Griffin, and D. M. Neumark, J. Chem. Phys. **123**, 231102 (2005).
[47] L. Turi, A. A. Mosyak, and P. J. Rossky, J. Chem. Phys. **107**, 1970 (1997).
[48] V. Herrmann and P. Krebs, J. Phys. Chem. **99**, 6794 (1995).
[49] P. Minary, L. Turi, and P. J. Rossky, J. Chem. Phys. **110**, 10953 (1999).
[50] X. Shi, F. H. Long, H. Lu, and K. B. Eisenthal, J. Phys. Chem. **99**, 6917 (1995).
[51] P. K. Walhout, J. C. Alfano, Y. Kimura, C. Silva, P. J. Reid, and P. F. Barbara, Chem. Phys. Lett. **232**, 135 (1995).
[52] C. Silva, P. K. Walhout, P. J. Reid, and P. F. Barbara, J. Phys. Chem. A **102**, 5701 (1998).
[53] A. Thaller, R. Laenen, and A. Laubereau, J. Chem. Phys. **124**, 024515 (2006).
[54] N. I. Hammer, J.-W. Shin, J. M. Headrick, E. G. Diken, J. R. Roscioli, G. H. Weddle, and M. A. Johnson, Science **306**, 675 (2004).
[55] A. V. Davis, R. Wester, A. E. Bragg, and D. M. Neumark, J. Chem. Phys. **118**, 999 (2003).
[56] A. T. J. B. Eppink and D. H. Parker, Rev. Sci. Instrum. **68**, 3477 (1997).
[57] V. Dribinski, A. Ossadtchi, V. A. Mandelstahm, and H. Reisler, Rev. Sci. Instrum. **73**, 2634 (2002).
[58] A. Kammrath, J. R. R. Verlet, A. E. Bragg, G. B. Griffin, and D. M. Neumark, J. Phys. Chem. A **109**, 11475 (2005).
[59] S. F. Fischer and W. Dietz, Z. Phys. Chem. **221**, 1 (2007).
[60] D. Borgis, P. J. Rossky, and L. Turi, J. Chem. Phys. **125**, 064501 (2006).